Molecular Cell, Vol. 8, 1313–1325, December, 2001, Copyright ©2001 by Cell Press

# Structural Characterization of the Intramolecular Interaction between the SH3 and Guanylate Kinase Domains of PSD-95

**Gisele A. Tavares, Ezequiel H. Panepucci, and Axel T. Brunger**[1]
The Howard Hughes Medical Institute and
Department of Molecular and Cellular Physiology
Department of Neurology and Neurological Sciences
and Stanford Synchrotron Radiation Laboratory
Stanford University
1201 Welch Road P210 MSLS
Stanford, California 94305

## Summary

**PSD-95/SAP90 is a member of the MAGUK superfamily. In excitatory synapses, PSD-95 clusters receptors and ion channels at specific sites in the postsynaptic membrane and organizes downstream signaling and cytoskeletal molecules. We have determined the crystal structures of the apo and GMP-bound forms to 2.3 and 2.0 Å resolutions, respectively, of a fragment containing the SH3, HOOK, and guanylate kinase (GK) domains of PSD-95. We observe an intramolecular interaction between the SH3 and GK domains involving the formation of a β sheet including residues N- and C-terminal to the GK domain. Based on amino acid conservation and mutational data available in the literature, we propose that this intramolecular interaction is a common feature among MAGUK proteins.**

## Introduction

Neurotransmission occurs when a neurotransmitter is released from a presynaptic cell in response to the arrival of an action potential, crosses the synaptic cleft, and reaches the postsynaptic cell. The postsynaptic membrane of excitatory synapses contains an electron-dense specialization called postsynaptic density (PSD) (Ziff, 1997), which is enriched in receptors, enzymes, signaling molecules, cytoskeleton components, and adhesion molecules all arranged to mediate synaptic transmission. Thus, the localization and degree of clustering of postsynaptic proteins to their sites of function are crucial for neurotransmission and may be involved in synaptic plasticity (Scannevin and Huganir, 2000; Migaud et al., 1998; Lüscher et al., 2000).

In excitatory synapses, the scaffold protein PSD-95/SAP90 (postsynaptic density-95/synaptic-associated protein 90), an abundant component of the PSD (Ziff, 1997), anchors ionotropic glutamate receptors and potassium channels in the PSD as well as organizes signaling molecules and cytoskeletal elements (Scannevin and Huganir, 2000; Sheng and Pak, 2000; Tomita et al., 2001). PSD-95 and its homologs (SAP97/hdlg, chapsyn-110/PSD-93, and NE-dlg/SAP102) comprise the membrane-associated guanylate kinase (MAGUK) superfamily (Cho et al., 1992; Kistner et al., 1993; Woods and Bryant, 1993; Stathakis et al., 1997). Members of the MAGUK superfamily are membrane-associated proteins that possess a conserved core containing three modules: a PSD-95/Dlg/ZO-1 (PDZ) domain, a Src homology 3 (SH3) domain, and a domain with homology to the enzyme guanylate kinase (GK) (Figure 1A) (Anderson, 1996; Fanning and Anderson, 1999; Dimitratos et al., 1999). Due to their modular nature, MAGUK proteins are well suited to mediate clustering of different proteins through protein-protein interactions involving each module. The specific protein-protein interactions can create protein microdomains near the plasma membrane (Dimitratos et al., 1999).

Although little is known about binding partners for the SH3 domain of MAGUK proteins, its importance has been demonstrated in *Drosophila*, where mutations in the SH3 domain of the MAGUK protein Dlg cause epithelial overgrowth and malignant transformation (Woods et al., 1996). SH3 domains are adaptor modules, present in many signaling and cytoskeletal proteins, that usually bind proline-rich peptides with the consensus sequence PXXP (Pawson and Scott, 1997; Xu et al., 1997; Sicheri et al., 1997). The only proline-rich binding partner for the SH3 domain of a MAGUK member that has been identified to date is the kainate subtype glutamate receptor subunit KA2, which binds to the SH3 domain of PSD-95 via its two C-terminal proline-rich sequences (Garcia et al., 1998).

The GK domain of PSD-95 does not have catalytic activity (Kistner et al., 1995) but rather directly binds to cytoplasmic proteins such as SAPAP/GKAP/DAP family members (Kim et al., 1997; Naisbitt et al., 1997; Takeuchi et al., 1997), BEGAIN (brain-enriched guanylate kinase-associated protein) (Deguchi et al., 1998), SPAR (a Rap-specific GTPase-activating protein) (Pak et al., 2001), and MAP1A, a microtubule binding protein (Brenman et al., 1998). Both the GK and SH3 domains of PSD-95 and SAP97 interact with the scaffold proteins AKAP79/150 (A-kinase anchoring protein) (Dodge and Scott, 2000; Colledge et al., 2000), which bind protein kinases A and C, as well as the phosphatase calcineurin in neurons (Colledge and Scott, 1999).

The HOOK domain that links the SH3 and GK domains is a fairly distinctive region among MAGUK proteins. In *Drosophila*, the HOOK domain localizes Dlg to the plasma membrane of imaginal discs and regulates epithelial growth (Hough et al., 1997). It is also required for correct targeting of Dlg to synaptic and septate junctions (Thomas et al., 2000). The MAGUK proteins CASK (Cohen et al., 1998), p55 (Marfatia et al., 1994), and SAP97 (Lue et al., 1994) bind the protein band 4.1 through the I3 region of the HOOK domain, thereby linking the plasma membrane to the actin/spectrin cytoskeleton. The second region of the HOOK domain consists of a short stretch of basic amino acids that binds calmodulin and mediates calmodulin-dependent dimerization of NE-dlg/SAP102 and PSD-95 (Masuko et al., 1999).

Using yeast two-hybrid assays, several MAGUK proteins, including PSD-95, chapsyn-110, SAP97, Dlg, CASK, and p55, were shown to form intra- or intermolecular interactions between the SH3 domain and the GK

[1] Correspondence: axel.brunger@stanford.edu

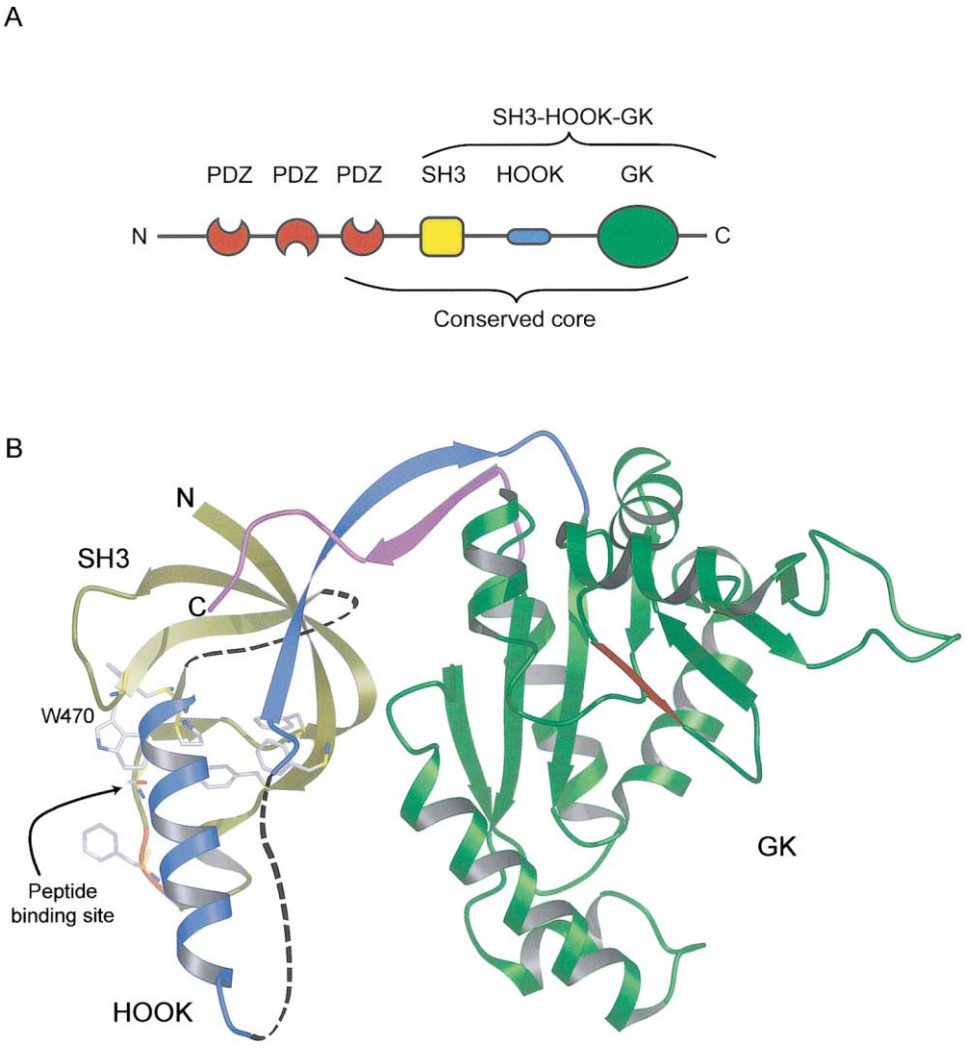


Figure 1. PSD-95 Domain Organization and Overall Architecture of PSD-95 SH3-HOOK-GK Domains

(A) PSD-95 domain organization showing the conserved core of MAGUK proteins and the fragment studied in this work (SH3-HOOK-GK).
(B) SH3-HOOK-GK model built using the GMP-bound structure and residues 439–445 and 502–508 from the apo form. In gold is shown the SH3 domain, in blue the HOOK domain, in green the GK domain, and in magenta the last 12 residues C-terminal to the GK domain. The dashed lines represent the disordered parts of the molecule in both crystal forms. The residues represented in the SH3 domain constitute the proline-rich peptide binding site. In red are shown the regions in the SH3 and GK domains that participate in crystallographic contacts in both crystal forms.

domain with a preference for intramolecular interactions (McGee and Bredt, 1999; Shin et al., 2000; Nix et al., 2000). Furthermore, the GK domain of hCASK binds the SH3 domain of hDlg and exhibits some specificity for these heterotypic interactions. For example, hDlg GK domain binds to its own SH3 domain but not to those of hCASK and p55 (Nix et al., 2000). Heterotypic interaction has also been shown in vitro between SH3 and GK domains of members of the PSD-95 family (Shin et al., 2000).

Interestingly, none of the GK domains from MAGUK proteins contain the consensus SH3 binding motif PXXP. The minimal segment of the GK domain of PSD-95 sufficient for SH3 interaction consists of the GK domain and some flanking residues at its N- and C termini, including about 20 residues preceding the N-terminal boundary of the GK domain and 13 residues C-terminal to the GK domain (McGee and Bredt, 1999; Shin et al., 2000). Additionally, mutations in *dlg* that resemble the truncation of the last 12 residues of the GK domain are lethal in *Drosophila* in the absence of maternal contribution (Woods et al., 1996). Mutational studies on the SH3 domain of MAGUK proteins suggested that the peptide binding site is not involved in the intramolecular interaction (McGee and Bredt, 1999; Shin et al., 2000; Nix et al., 2000). On the other hand, a mutation in the SH3 domain that produced a severe tumorogenic phenotype in flies (Woods et al., 1996), corresponding to Leu460Pro in PSD-95, was sufficient to disrupt the intramolecular interaction (McGee and Bredt, 1999; Shin et al., 2000).

Functional evidence regarding the intramolecular interaction comes from the study of PSD-95 and $K^+$ channels. Disruption of the intramolecular interaction does not interfere with the ability of PSD-95 to bind $K^+$ channels, but it does abolish the clustering activity of PSD-95 (Shin et al., 2000). Therefore, it has been suggested that the targeting and clustering activity of PSD-95 may be controlled by the regulation of the intramolecular interaction (Shin et al., 2000).

In this paper, we report the three-dimensional structures of the 430–724 fragment of PSD-95, including the SH3, HOOK, and GK domains at 2.3 Å and 2.0 Å resolutions for the apo and GMP-bound forms, respectively. Our structure provides unexpected findings to the interactions between these MAGUK domains. The SH3 and GK domains share the conserved topology of their homologs. Binding of GMP to the GK domain of PSD-95 did not induce large conformational changes in the nucleoside binding domain, in contrast to yeast guanylate kinase (Blaszczyk et al., 2001). The intramolecular interaction between the SH3 and GK domains occurs via the formation of an antiparallel two-stranded β sheet, where residues C-terminal of the HOOK region form one strand, and the last 12 residues C-terminal to the GK domain form the other. Hydrophobic interactions along with hydrogen bonds make up the interface between the domains. The proline binding site of the SH3 domain is not involved in the intramolecular interaction. The conservation of the amino acids involved in interactions at the interface as well as those involved in the formation of the β sheet, along with mutational data available regarding the intramolecular interaction, suggests that the SH3-HOOK-GK intramolecular interaction is a general feature of MAGUK proteins.

## Results

### Structure Determination

Recombinant rat SH3-HOOK-GK of PSD-95 comprising residues from 430 to 724 plus five cloning residues at the N terminus was expressed in *E. coli*, purified to homogeneity, and crystallized by vapor diffusion. The GMP-bound form crystallized in spacegroup $P4_12_12$ and diffracted to $d_{min} = 2.0$ Å, whereas the apo form crystallized in spacegroup P1 with $d_{min} = 2.3$ Å. Seleno-methionine substitution was carried out in order to solve the GMP-bound crystal structure ($P4_12_12$ crystal form) using multiwavelength anomalous diffraction (MAD) phasing (Hendrickson, 1991) (Table 1). Of the three Se sites found by the CNS automated Patterson search method (Grosse-Kunstleve and Brunger, 1999), two were well-ordered and were useful for MAD phasing. After density modification with solvent flipping (Abrahams and Leslie, 1996) and histogram matching (Zhang and Main, 1990), phases were extended to 2.0 Å resolution. The resulting map was of excellent quality (Figure 6B). The final model was refined to an $R_{free}$ value of 26.2 % and includes residues 430 to 439, 445 to 476, 486 to 502, and 520 to 724. The remaining residues could not be observed in both experimental and annealed omit electron density maps and were omitted from the final model. The apo crystal structure with two molecules in the asymmetric unit (P1 crystal form) was solved to 2.3 Å resolution by molecular replacement using as search models domains of the refined structure of the GMP-bound form. The final model, refined to an $R_{free}$ value of 26.3%, includes residues 430 to 476, 485 to 508, 520 to 568, 578 to 603, and 606 to 720. The remaining residues were not visible in electron density maps and were omitted from the final model.

### The SH3 Domain

The SH3 domain of PSD-95 (residues 430 to 490) shares about 30% similarity with other SH3 domains. The arrangement of the four β strands that form the β sandwich is similar to that of other SH3 domains (Xu et al., 1997; Sicheri et al., 1997) (Figure 1B). However, the fifth β strand is composed of residues from 522 to 531 of the HOOK domain. The polyproline peptide binding site, which is highly conserved among the SH3 domains, is composed of a cluster of hydrophobic residues comprising Phe437, Tyr439, Phe447, Phe454, Trp470, and Pro489, which are conserved in different MAGUK families of proteins (Figure 2). In both apo and GMP-bound structures, the SH3 peptide binding site does not participate in the SH3-HOOK-GK intramolecular interaction but rather is exposed to the surface. Along with residues composing the interface between the two domains, Phe454, present in the canonical n-Src loop that connects the second and third β strands, interacts with residues Phe688 and Ile691 in the GK domain. The canonical RT loop, which connects the first and second β strands, is not facing the GK domain. On the other hand, this loop forms a three residue β sheet with a crystallographically related GK domain, involving residues Gly446 to Leu448 of the SH3 domain and Glu600 to Gly602 of the GK domain (Figure 1B). Interestingly, this interaction is seen in both molecules in the asymmetric unit of the apo form as well as in the GMP-bound crystal form.

### The HOOK Domain

The HOOK domain comprises residues 491 to 533, which are located between the SH3 and GK domains (Figures 1B). In the SH3-HOOK-GK apo structure, the N-terminal portion of the HOOK region forms an 18 residue α helix (491 to 508) between the forth and fifth canonical β strands of the SH3 domain. The same helix is present in the GMP-bound crystal form, though only about half of it is ordered and it forms a different angle with the rest of the structure (Figure 4A). Superposition of the SH3 domain of the apo and GMP-bound structures shows that the N terminus of the helix is flexible, being farther away from the SH3 domain in the apo form. The different conformation of this helix in both structures is due to differences in crystal packing. In both the apo and GMP-bound structures, the helix has a cluster of basic residues on one side, giving it an amphipathic character (Figure 3A). Residues Ser522 to Val531 in the HOOK domain form the fifth β strand of the SH3 domains (Figure 1B).

### The GK Domain

Nucleoside monophosphate kinases (NMP kinases) are composed of three dynamic domains: CORE, LID, and NMP binding domains. For yeast guanylate kinase, both the NMP and LID domains undergo large conformational changes upon binding of ligands, such as nucleoside

Table 1. Crystallographic Data, Phasing Statistics, and Refinement Statistics

| | | Cell Dimensions | | | | | |
|---|---|---|---|---|---|---|---|
| Dataset | Space Group | a (Å) | b (Å) | c (Å) | α(°) | β(°) | γ(°) |
| Native (GMP) | P $4_1$ $2_1$ 2 | 59.72 | 59.72 | 209.96 | 90.00 | 90.00 | 90.00 |
| SeMet (GMP) | P $4_1$ $2_1$ 2 | 59.42 | 59.42 | 210.64 | 90.00 | 90.00 | 90.00 |
| Native (Apo) | P1 | 45.01 | 53.41 | 63.26 | 89.96 | 90.00 | 91.78 |

Data Statistics

| Crystal | $d_{min}$ (Å) | Total Number of Reflections | Average Redundancy | Completeness (%) | I/σ | $R_{sym}$ (%)[a] |
|---|---|---|---|---|---|---|
| SeMet $\lambda_1$ (0.978996 Å) | 2.6 | 23805 | 4.6 (4.1) | 98.4 (92.6) | 17.9 | 5.0 (26.6) |
| SeMet $\lambda_2$ (0.904964 Å) | 2.6 | 24661 | 4.9 (4.7) | 99.0 (99.0) | 17.3 | 5.0 (28.5) |
| Native (0.964818 Å) | 2.0 | 26060 | 6.6 (7.0) | 97.5 (98.8) | 24.3 | 4.2 (13.5) |
| P1 (0.964818 Å) | 2.3 | 25724 | 3.0 (3.0) | 98.4 (97.6) | 15.7 | 4.3 (10.2) |

MAD Phasing Statistics (26.95–2.59 Å; High Resolution Bin 2.71–2.59 Å)[b,c]

| | $\lambda_1 \rightarrow \lambda_1^-$ | $\lambda_1 \rightarrow \lambda_2^+$ | $\lambda_1 \rightarrow \lambda_2^-$ |
|---|---|---|---|
| Phasing power | 0.84 (0.20) | 0.57 (0.17) | 0.91 (0.22) |
| Figure-of-merit | 0.19 (0.02) | 0.19 (0.03) | 0.24 (0.04) |
| Overall figure-of-merit | 0.37 (0.07) | | |

Refinement Statistics

| | GMP-Bound | Apo |
|---|---|---|
| Luzzati coordinate error (Å) | 0.27 | 0.28 |
| Cross-validated Luzzati coordinate error (Å) | 0.31 | 0.35 |
| Bond length deviation (Å) | 0.01 | 0.01 |
| Bond angle deviation | 1.15° | 1.14° |
| Improper angle deviation | 0.70° | 0.65° |
| Dihedrals | 22.5° | 22.3° |
| B factors: min, average, max (Å$^2$) | 21.68, 37.09, 69.73 | 11.12, 28.69, 55.84 |
| Residues in core regions (%) | 92.8 | 94.0 |
| Residues in disallowed regions (%) | 0.4 | 0.4 |
| Number of reflections (test set) | 42653 (4621) | 22943 (2513) |

Values in parentheses are for the high resolution bin: 2.71–2.59 Å for the SeMet GMP-bound, 2.03–2.00 Å for the native GMP-bound, 2.38–2.30 Å for the native apo form.

[a] $R_{sym} = \Sigma_h \Sigma_i |I_i(h) - \langle I(h) \rangle| / \Sigma_h \Sigma_i I_i(h)$ where $I_i(h)$ is th i$^{th}$ measurement and $\langle I(h) \rangle$ is the mean of all measurements of $I(h)$ for Miller indices $h$.

[b] Values are $\langle (\Delta|F|)^2 \rangle^{1/2} / \langle |F|^2 \rangle^{1/2}$ where $\Delta|F|$ is the dispersive (off-diagonal elements), Bijvoet difference (diagonal elements), computed between 500–2.6 Å.

[c] MAD phasing power is defined as $[\langle |F_D - F_N|^2 \rangle / \int P(\phi)(||F_N| \, e^{\phi} + \Delta F_h| - |F_D|)^2 d\phi]^{1/2}$ where $P(\phi)$ is the experimental phase probability distribution. $F_N$ corresponds to the structure factors at the reference wavelength $\lambda_1$ and $F_D$ corresponds to the structure factors at wavelength $\lambda_i$ (indicated by a superscript +) or its Friedel mate (indicated by a superscript −), and $\Delta F_h$ is the difference in the heavy atom structure factors between the two wavelengths.

monophosphates and ATP, respectively. The GK domain of PSD-95 (residues 534 to 713) shares about 35% identity with yeast guanylate kinase. The CORE domain is composed of five parallel β strands (β6, β7, β12, β13, and β14) and six α helices (α2, α4, α5, α6, α7, and α8) (Figures 2 and 4B). The NMP domain is composed of four β strands (β8, β9, β10, and β11) and one α helix (α3), which together form the GMP binding site. The LID domain is the loop between the CORE α6 and α7 helices. Superposition of the apo and GMP-bound CORE domains shows a root mean square difference (rmsd) of 0.31 Å for 139 superposed $C_\alpha$ atoms, while greater differences are seen in the NMP binding site, with an rmsd of 1.28 Å when 35 $C_\alpha$ atoms are superimposed (Figure 4B). Superposition of the LID domain of the apo and GMP-bound forms showed an rmsd of 0.26 Å when six $C_\alpha$ atoms are superposed. The interactions with GMP are shown in detail in Figure 5. Atoms N1 and N2 from the guanine ring form hydrogen bonds with Asp629 from the CORE domain. The phosphate group forms three hydrogen bonds with Arg568 and Arg571, from the loop between β8 and β9. Tyr580 forms one hydrogen bond with O2P of the phosphate group, Tyr604 is involved in a hydrophobic contact, and Tyr609 forms one hydrogen bond with O1P of the phosphate group.

In the GMP binding site, an MPD (2-methyl-2,4-pentanediol) molecule was found between the guanine ring and the main chain of β10 (Figure 5). Two guanidine molecules are also near to the GMP binding site, facing the solvent. One of the two guanidines forms a hydrogen bond with Asp579, which is located in the end of the loop between β8 and β9, whereas the other guanidine is closer to the GMP, forming a hydrogen bond with O3P of the phosphate group and a hydrogen bond with an Asp residue of a neighboring molecule. In the apo structure, the loop between β8 and β9 is disordered in both molecules in the asymmetric unit. This region in the GMP-bound structure interacts either with guanidine, GMP, or MPD, which probably contributes to their ordering in this crystal form.

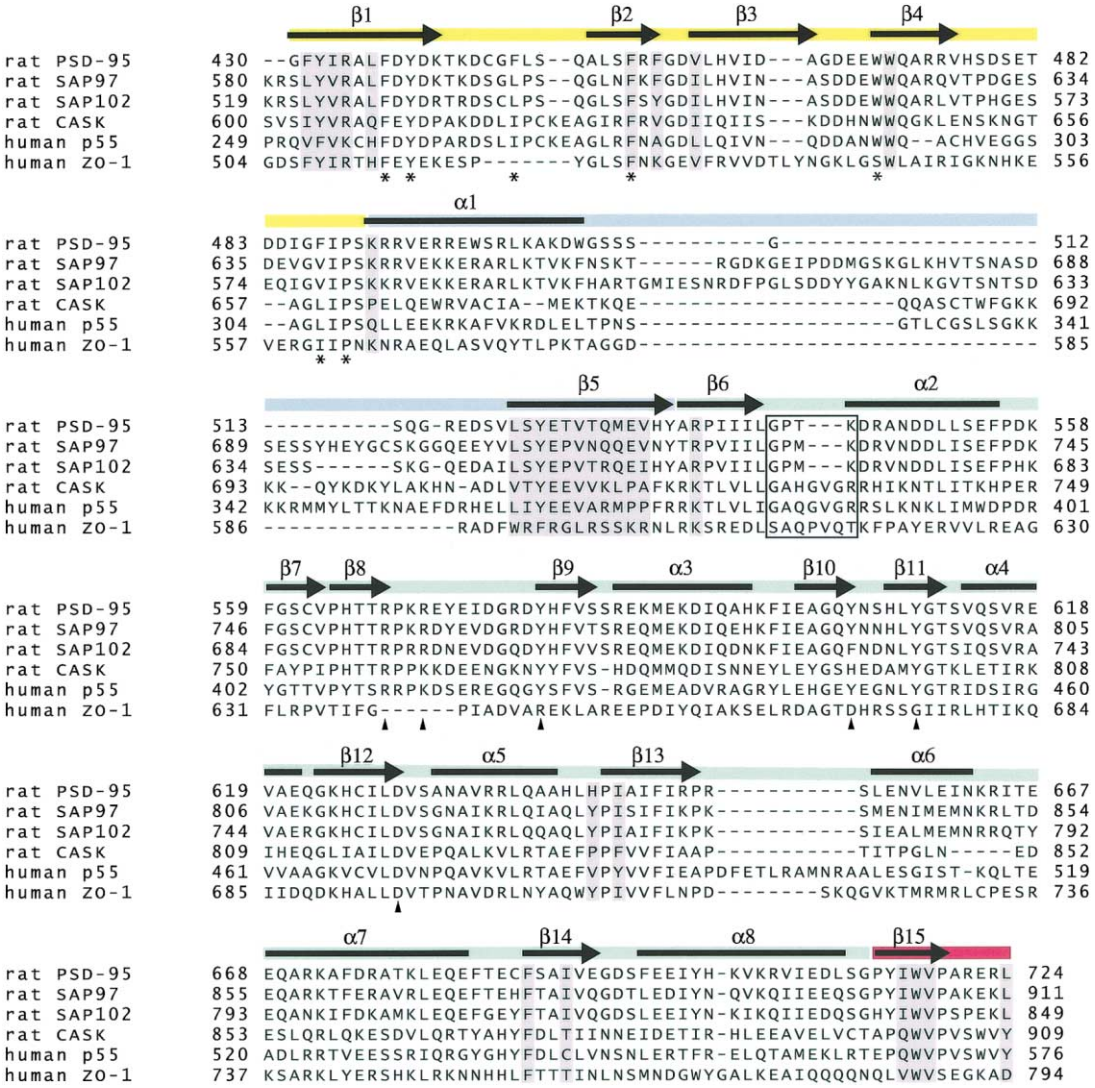


Figure 2. Sequence Alignment of PSD-95 to Other MAGUK Proteins

Rat PSD-95 SH3-HOOK-GK fragment aligned with rat SAP97/hDlg, rat NE-dlg/SAP102, rat CASK, human p55, and human ZO-1 (zona occludens-1). Sequences were aligned using ClustalW (Thompson et al., 1994). Yellow indicates the SH3 domain, blue the HOOK domain, green the GK domain, and magenta the C-terminal tail. The secondary structure is indicated in the top line as arrow for β sheet and solid line for α helix. The residues colored in gray are involved in the intramolecular interaction. Residues tagged with a star belong to the proline-peptide binding site of the SH3 domain, and residues tagged with a triangle are involved in the binding of GMP in the GK domain. The boxed residues constitute the ATP binding motif.

### Intramolecular Interactions

The intramolecular interactions between the SH3, HOOK, and GK domains consist of a seven residue antiparallel β sheet and a cluster of hydrophobic residues from the different domains and the C-terminal tail. Residues Thr526 to Val531 of the HOOK domain form the antiparallel β sheet with residues Pro714 to Val718, just C-terminal to the GK domain (Figure 6C). In both the apo and GMP-bound forms, the same interaction is observed, though residues Arg721 to Leu724 are not seen in the electron density map of the apo form. At the interface of the SH3, HOOK, and GK domains, Arg434 (SH3) forms a hydrogen bond with the carbonyl group of the main chain of residue Phe688 between α6 and β12 of the GK domain (Figure 6F). A hydrophobic core is formed between the three domains, consisting of residues from the SH3 domain (Phe431, Tyr432, Ile433, Arg434, Leu436, Phe456, Val459, Trp471, and Val476), the HOOK domain (Lys491, Leu521, Tyr523, Thr525, Val526, Gln528, Met529, Val531, and Arg535), the GK domain (His644, Ile646, Thr685, Phe688, Ile691); and the C-terminal tail (Ile716, Trp717, Val718, and Leu724) (Figures 6D and 6E). Their conservation among different MAGUK proteins is shown in Figure 2. Water molecules are present at the interface bridging residues via hydrogen bonds among the different domains. The two crystal forms have nine water molecules structurally conserved at this interface.

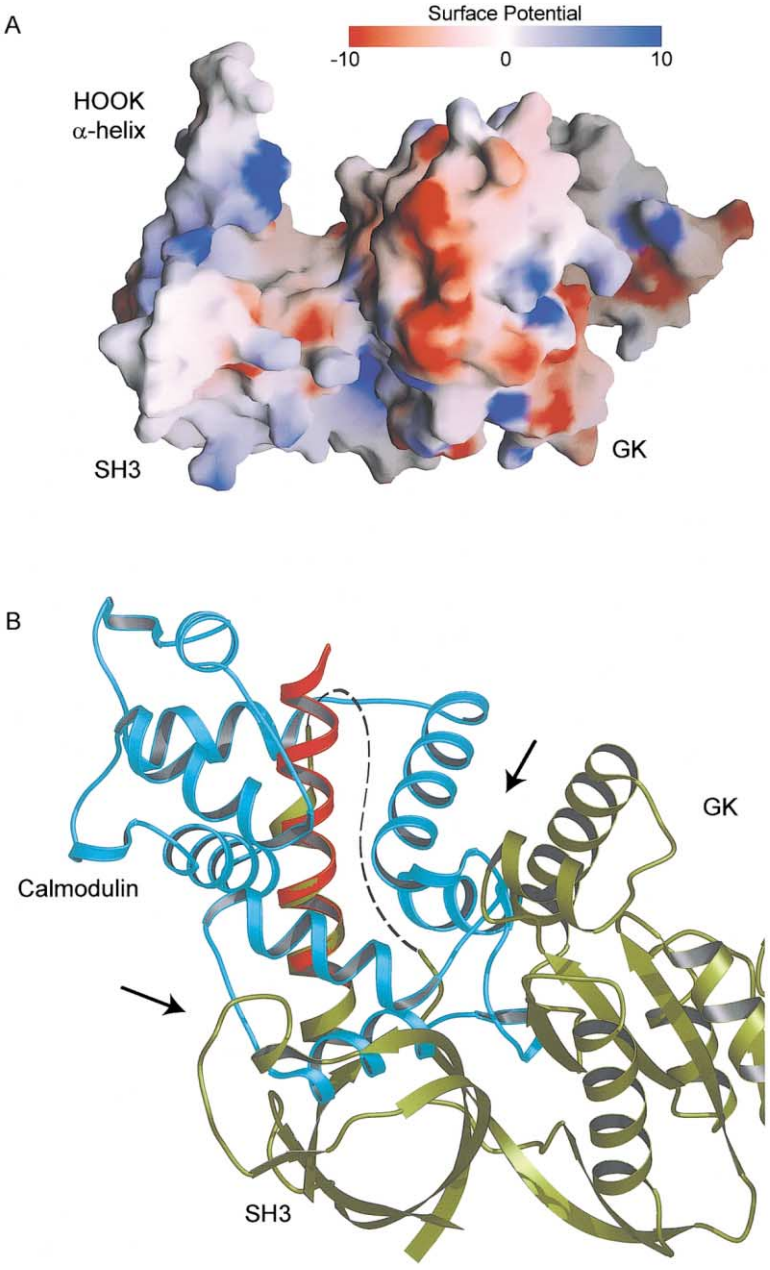


Figure 3. Electrostatic Potential at the Molecular Surface and the Steric Hindrance between Calmodulin and PSD-95

(A) Electrostatic potential at the molecular surface of PSD-95 depicting the characteristic patch of basic amino acids in the HOOK α helix (figure produced with GRASP, Nicholls et al., 1993).

(B) Superposition of smooth muscle myosin light chain kinase peptide complexed with calmodulin and PSD-95 HOOK α helix showing clashes (indicated by arrows) that occur between calmodulin and SH3-HOOK-GK. Calmodulin is shown in cyan, the superimposed helices in red/gold, and PSD-95 SH3-HOOK-GK in gold. The dashed line represents the disordered part of the molecule in both crystal forms. The SH3-HOOK-GK structure shown is a model built using the GMP-bound structure and residues 502–508 from the apo form.

## Discussion

The proline-rich peptide binding site of the SH3 domain of PSD-95 is exposed at the surface of the molecule away from the intramolecular SH3-HOOK-GK interaction and would be accessible to bind its partners (Figure 1B). The SH3 domain of PSD-95 binds and clusters members of the kainate subgroup of glutamate receptors. The coexpression of the receptors with PSD-95 resulted in cells making long-lasting glutamate responses caused by changes in desensitization (Garcia et al., 1998). The KA2 subunit binds to the SH3 domain via its two proline-rich sequences at the C-terminal tail. Recently, another binding partner for the SH3 domain of PSD-95 has been identified as AKAP79/150 (A-kinase anchoring protein), though the mode of interaction remains unknown (Colledge et al., 2000). The intramolecular interaction does not seem to be a regulator of the SH3 domain binding ability.

The GK domain of members of the MAGUK family is homologous to the enzyme guanylate kinase that converts GMP to GDP using ATP as the phosphate donor. Authentic enzymes have conserved GMP and ATP binding sites, whereas members of the MAGUK family have diverged at the phosphate binding sites. While some MAGUK proteins have both sites conserved (p55 and CASK), the entire PSD-95 family has only a conserved GMP binding site (Figure 2). Catalytic activity has only been demonstrated for a bacterially expressed p55-GST fusion protein; this activity was 190 times lower than that of porcine guanylate kinase (Dimitranos et al., 1999). Guanylate kinase activity has been tested for PSD-95

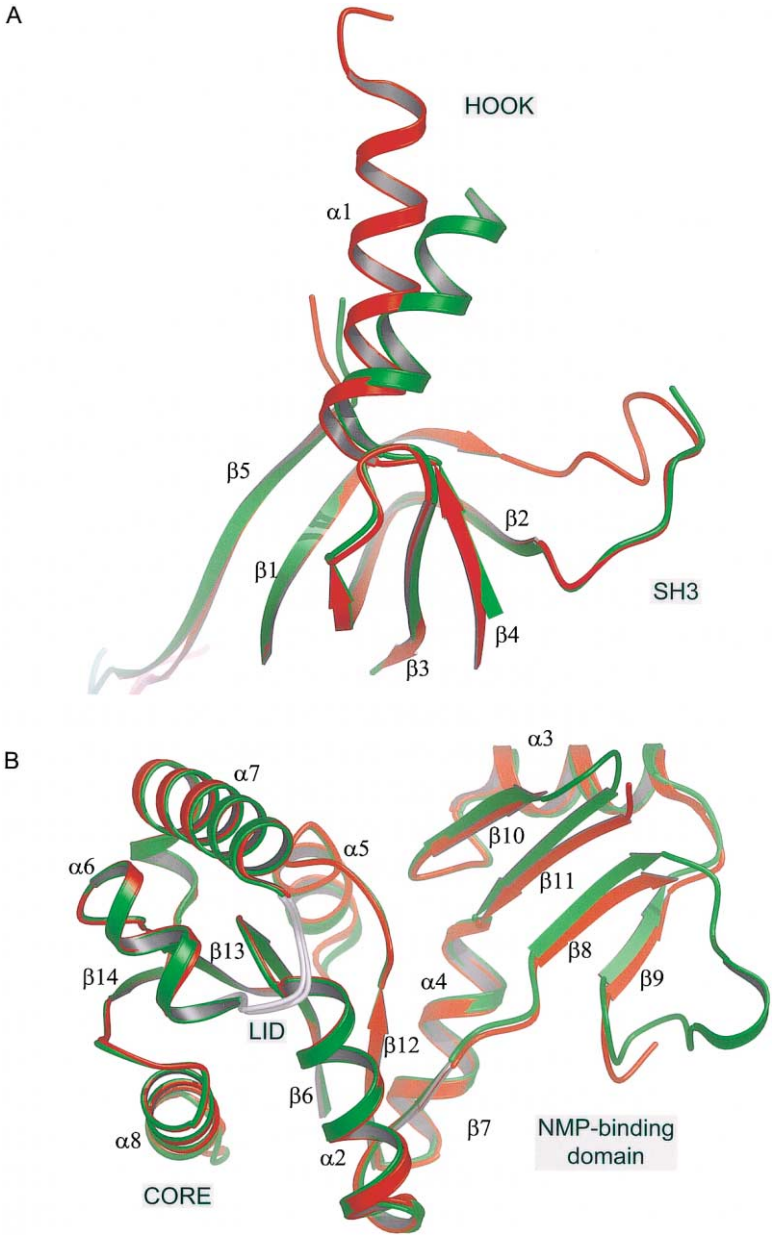


Figure 4. Superposition of the Apo and GMP-Bound SH3-HOOK and GK Domains

(A) Superposition of the SH3 domains of the GMP-bound (green) and apo (red) structures showing the movement of the HOOK α helix.
(B) Superposition of the CORE domains of the GMP-bound (green) and apo (red) structures showing only a slight movement of the NMP binding domain. The LID domain is shown in gray for both crystal forms.

and SAP97 (Kistner et al., 1995; Kuhlendahl et al., 1998), and in both cases no enzymatic activity was detected. Ten of eleven amino acid residues involved in the binding of the GMP in the yeast enzyme are conserved in PSD-95, which has a dissociation constant for GMP in the micromolar range (Kistner et al., 1995). Although the conservation of the residues involved in the binding of GMP is high, the number of residues interacting directly with GMP in the PSD-95 crystal structure is smaller than that seen in the yeast guanylate kinase (six contacts in PSD-95 versus nine in yeast guanylate kinase).

The only difference between the apo and GMP-bound crystallization conditions was the presence of guanidine, an additive screened in order to obtain high-quality diffracting crystals. GMP binding was only observed when guanidine was present in the crystallization condition, and indeed a guanidine molecule bound near the GMP binding site forms a hydrogen bond with O3P of the phosphate group and a hydrogen bond with an Asp residue from a crystallographically related molecule. This guanidine molecule might mimic a guanidine group from an arginine residue of a putative binding partner. GMP binding would help to stabilize the loop between β8 and β9, promoting the binding of a target protein to that region.

Binding of GMP to the GK domain of PSD-95 induced much smaller conformational changes in the NMP binding site than those observed in the yeast guanylate kinase (Blaszczyk et al., 2001). In the yeast enzyme, GMP binding promotes the movement of the NMP binding site toward the active center of the enzyme as well as the opening of the LID domain in order to make space for ATP. The lack of large conformational changes upon binding of GMP agrees with the absence of enzymatic

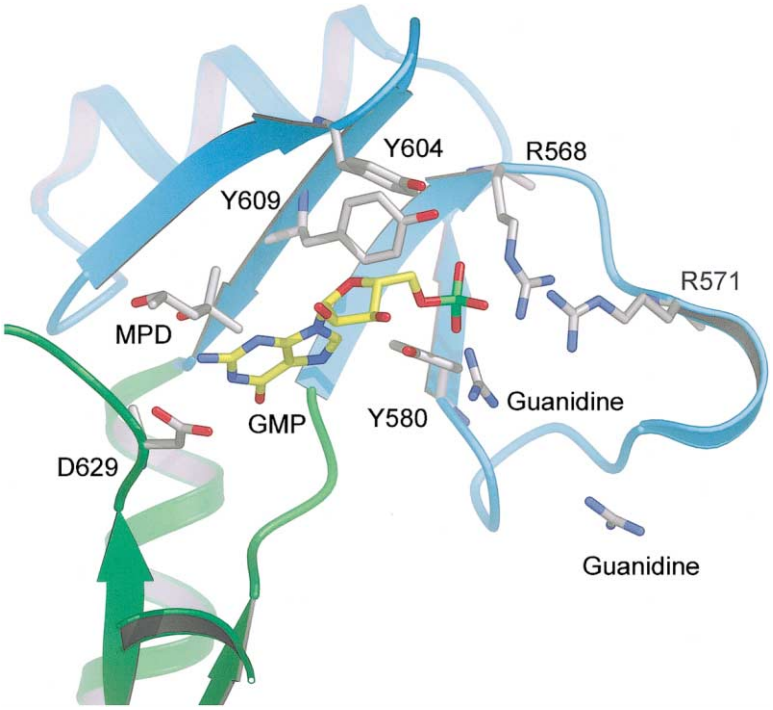


Figure 5. GMP Binding Site of PSD-95

GMP (yellow carbon atoms) binds to the GK NMP binding domain (cyan ribbon). This interaction appears to be stabilized by an MPD molecule. The binding residues (white carbon atoms) are shown as well as two guanidine molecules.

activity of the PSD-95 GK domain and supports the idea that GMP might act as a cofactor for the binding to another protein.

The HOOK α helix seems to be flexible, being closer to the SH3 domain in the GMP-bound structure. In the apo form, the HOOK α helix is further away from the rest of the molecule. This helix forms crystal contacts with neighboring molecules, which accounts for its ordering in this crystal form. The basic residues in the HOOK α helix (Lys491, Arg492, Arg493, Arg496, Arg497, Arg501, and Lys503 in PSD-95) are conserved among SAP97/hdlg, chapsyn-110/PSD-93, and NE-dlg/SAP102 (Figure 2). This region of NE-dlg/SAP102 interacts with calcium/calmodulin, suggesting that calmodulin may be able to interact with all of these MAGUK proteins (Masuko et al., 1999). Furthermore, by binding to NE-dlg/SAP102, calcium/calmodulin mediates the interaction between NE-dlg/SAP102 and PSD-95 (Masuko et al., 1999). Many calmodulin binding partners are characterized by the presence of a basic α helix of approximately 20 residues (Rhoads and Friedberg, 1997). Superposition of an α-helical fragment from smooth muscle myosin light chain kinase bound to calcium/calmodulin (PDB code: 1CDL) (Meador et al., 1992) with the PSD-95 HOOK α helix showed that clashes would occur between one lobe of calmodulin and the SH3 and GK domains of PSD-95 in both crystal forms, preventing binding (Figure 3B). Furthermore, the region in the HOOK domain between the α helix and the following β strand, which is disordered in both PSD-95 crystal structures, presumably would not allow the binding of calmodulin to the amphipathic α helix in the conformation seen in these crystal structures. Our attempts to bind calmodulin to the SH3-HOOK-GK fragment of the PSD-95 failed, in agreement with our modeling. One possible way for calmodulin to interact with PSD-95 would be the displacement of the GK domain, along with the region preceding it. This would lead to the disruption of the intramolecular interaction and/or the interface between the domains, and consequently to exposure of the α helix. The conformational variablility of the helix (Figure 4A) supports this idea. However, it is possible that NE-dlg/SAP102 binds calcium/calmodulin due to its longer HOOK domain, which has an insertion of 45 amino acids following the α helix, relative to PSD-95 (Figure 2).

There is a wealth of biochemical data about the intramolecular and intermolecular interactions between SH3 and GK domains of different MAGUK proteins, such as PSD-95, CASK, hDlg, and p55 (McGee and Bredt, 1999; Shin et al., 2000; Nix et al., 2000). The intramolecular interaction between SH3 and GK domains of MAGUK proteins was characterized by mutational studies, with complete agreement among the data from different MAGUK proteins (McGee and Bredt, 1999; Shin et al., 2000; Nix et al., 2000). Mutation of Trp470 of PSD-95, a conserved residue in SH3 domains involved in peptide binding, to a phenylalanine or alanine, which is known to disrupt the SH3-proline-containing peptide interactions, did not abolish the intramolecular interaction (McGee and Bredt, 1999; Shin et al., 2000), while it did affect the intermolecular interaction (Shin et al., 2000). This observation can be explained by our crystal structures since Trp470 is part of the peptide binding site and does not participate in the intramolecular interaction (Figure 1B). This suggested that an intermolecular interaction might involve a different region of the SH3 domain. Mutation of residue Leu460 to Pro in PSD-95, the same mutation that produces a severe tumorogenic phenotype in *Drosophila* (Woods et al., 1996), led to the disruption of the intramolecular interaction (McGee and Bredt, 1999; Shin et al., 2000; Nix et al., 2000). In the crystal structure, Leu460 is located in the middle of the third β strand of

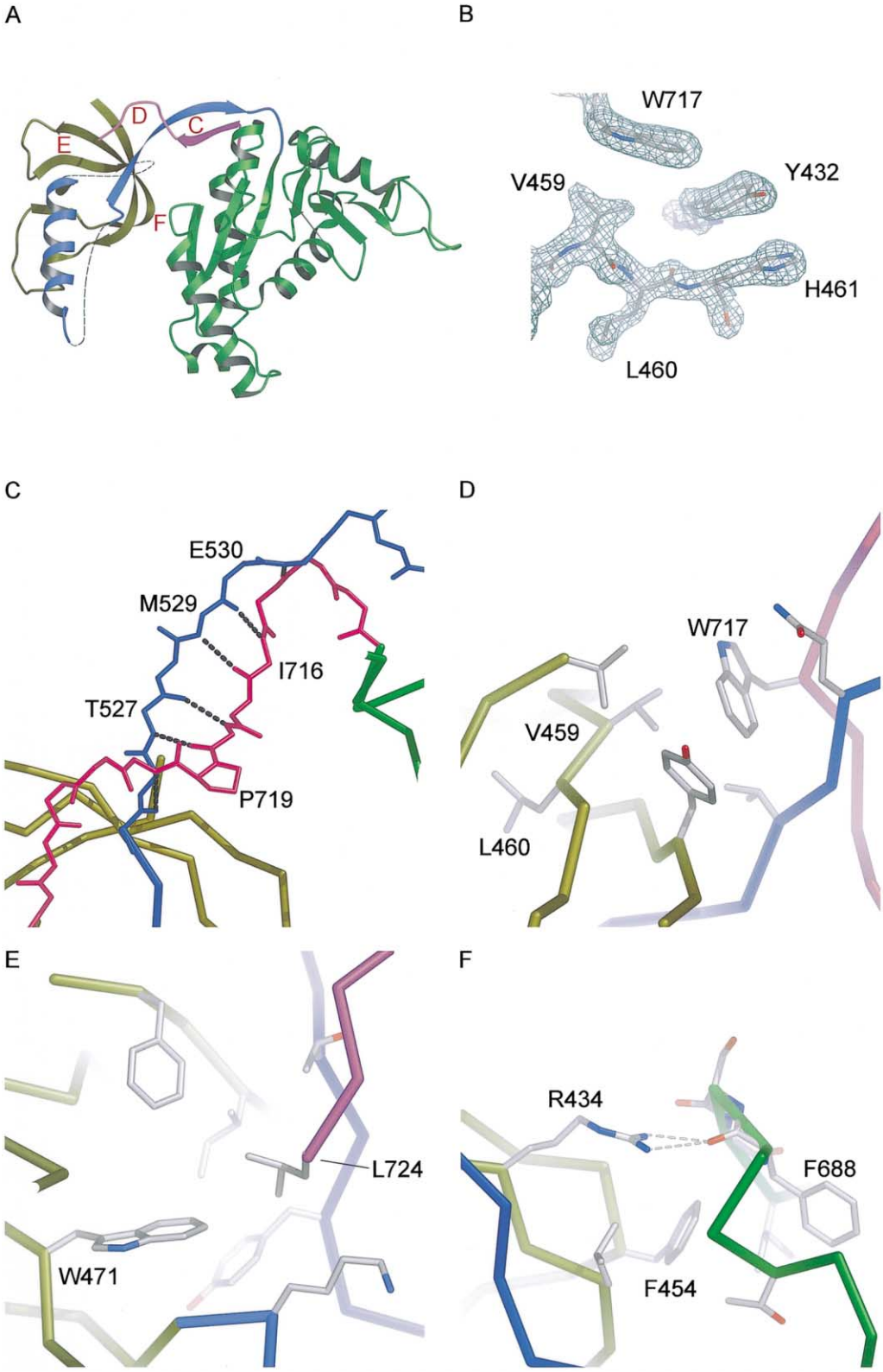


Figure 6. The SH3-HOOK-GK Intramolecular Interactions

(A) Overall representation of the SH3-HOOK-GK domains of PSD-95; red letters indicate the specific interactions depicted in the following panels: (B) representative $2F_o–F_c$ electron density map contoured at 1.5 $\sigma$ using combined model and experimental MAD phases around Val459; (C) the dashed black lines show the antiparallel $\beta$ sheet formed between the residues of the HOOK domain and the C-terminal tail. Hydrophobic interactions involving: (D) Trp717 from the C-terminal tail, (E) the C-terminal residue Leu724, and (F) hydrogen bond between Arg434 from the SH3 domain and carbonyl of Phe688 of the GK domain.

the SH3 domain positioned toward the interior of the β sandwich participating in extensive hydrophobic contacts (Figure 6D). The mutation of Leu460 to Pro might affect the positioning of neighboring residues including Val459, which faces Trp717 in the C-terminal tail. A less direct effect of destabilizing the third β strand might be the disruption of the interaction between His461 and Tyr432, which in turn faces Trp717.

Deletion of the last 12 residues C-terminal to the GK domain disrupts the intramolecular interaction between the SH3 and GK domains of PSD-95 (Shin et al., 2000). In the crystal structure of the 12 residues, seven are involved in the formation of the β sheet, and most of them participate in important hydrophobic interactions with residues from the SH3 and HOOK domains. Also, the C-terminal leucine is buried within the SH3 hydrophobic core (Figure 6E). Interestingly, cells transfected with both the $K^+$ channel Kv1.4 and either PSD-95, PSD-95 (L460P), or PSD-95ΔC (missing the last 13 amino acids) showed similar coimmunoprecipitation of the $K^+$ channel with PSD-95 antibodies. This indicates that the disruption of the intramolecular interaction did not have a deleterious effect on the ability of PSD-95 to bind to the channel. On the other hand, surface-associated coclusters of Kv1.4 and PSD-95 did not form when disruption of the intramolecular interaction took place, suggesting a regulatory role for the SH3-GK interaction in the ion channel-clustering activity of PSD-95 (Shin et al., 2000).

The crystal structures of PSD-95 reveal novel intramolecular interactions between the SH3 and GK domains. The intramolecular interaction between the SH3 and GK domains of PSD-95 does not involve the polyproline binding site of the SH3 domain, in contrast to the interaction between the SH3 and tyrosine kinase of the Src family of nonreceptor tyrosine kinases. This interaction involves the binding of the linker between the SH2 and the tyrosine kinase domains to the polyproline binding site of the SH3 domain, keeping the kinase in a catalytically inactive state (Xu et al., 1997; Sicheri et al., 1997). Based on the mutational analyses and the conservation of the residues involved in the intramolecular interaction (Figure 2), we propose that the intramolecular interaction observed in both the apo and GMP-bound forms of PSD-95 is a conserved feature among MAGUK proteins.

The intramolecular interactions between the SH3, HOOK, and GK domains in SAP97 interfere with GKAP binding (Wu et al., 2000), whereas a similar effect has not been observed in PSD-95. SAP97 contains an insertion relative to PSD-95 of 35 residues in the region between the HOOK α helix and the β strand seen in PSD-95 (Figure 2). Assuming that the same intramolecular interaction seen in the PSD-95 crystal structures takes place in SAP97, the same disposition of the domains seen in PSD-95 would be expected for SAP97. Therefore, we might predict that the insertion of 35 additional residues in the HOOK domain might create steric hindrance with α7 of the GK domain. From this analysis, one might infer a putative binding site for GKAP involving the α7 of the GK domain.

In summary, the crystal structures of the SH3-HOOK-GK domain of the PSD-95, in the apo and GMP-bound forms, show extensive intramolecular interactions between the individual domains of the protein. An intramolecular interaction occurs due to the formation of a β sheet involving residues N- and C-terminal to the GK domain and a hydrophobic core involving residues from the SH3, HOOK, and GK domains, as well as the C-terminal tail. We propose that these intramolecular interactions are a conserved feature of members of the MAGUK superfamily, based on mutational data available for different MAGUK proteins and conservation of the residues involved in the intramolecular interaction. We also propose that the intramolecular interaction could act as a molecular switch by regulating interactions with other factors such as calmodulin.

## Experimental Procedures

### Cloning, Expression, and Purification

DNA encoding the full-length rat PSD-95 was cloned from rat brain cDNA library (CLONTECH) using PCR with the following primers, 5′–3′: GCATTGGCTAGCATGGACTGTCTCTGTATA and GCCGAAT TCTCAGAGTCTCTCTCGGGCTGG. Subsequently, the full-length gene was used as template for the subcloning of the fragment corresponding to residues 430 to 724 into the pET28a vector. The resulting protein contained a thrombin-cleavable N-terminal hexahistidine tag. All DNA sequences were verified by dideoxynucleotide sequencing (Life Technologies). The recombinant native protein was expressed in bacterial strain BL21(DE3)* (Invitrogen) using Terrific Broth medium after induction with 0.1 mM isopropyl thio-β-D-galactopyranoside (American Bioanalytical) for 12 hr at 20°C. For the selenemethionine protein, cells were grown in M9 minimal medium containing 50 mg/l kanamycin at 37°C. At an optical density at 600 nm of 1.5, methionine synthesis was inhibited by the addition of 100 mg/l L-lysine, 100 mg/l L-phenylalanine, 100 mg/l L-threonine, 50 mg/l L-leucine, 50 mg/l L-isoleucine, 50 mg/l L-valine, and 60 mg/l D/L-selenomethionine (Sigma). After 15 min, cells were induced with 0.1 mM isopropyl thio-β-D-galactopyranoside (American Bioanalytical) for 12 hr at 20°C. For both native and selenomethionine preparations, cells were harvested and resuspended in Buffer A (20 mM Tris [pH 8.0], 200 mM NaCl, 15 mM β-mercaptoethanol, antipain 2 μg/ml, leupeptin 1 μg/ml, benzamidine 10 μg/ml, and aprotinin/Trasolyl 2 μg/ml), then lysed using a cell disrupter at 20,000 psi. The lysate was centrifuged for 45 min at 125,171 × g. The supernatant was incubated with 25 ml of Ni-NTA resin (Qiagen) under agitation at 4°C for 1 hr. After a wash of the beads with Buffer A + 20 mM imidazole (pH 8.0), a 150 ml gradient was run from Buffer A + 20 mM imidazole (pH 8.0) to Buffer A + 300 mM imidazole (pH 8.0). Fractions containing SH3-HOOK-GK domains (as visualized by Coomassie blue-stained SDS-PAGE gel) were pooled, and thrombin (Sigma) was added at 16 mg/l. The mixture was dialyzed overnight against buffer B (20 mM Tris [pH 8.0], 75 mM NaCl, and 2 mM dithiothreitol for native protein or 10 mM in the case of the selenomethionine protein). After dialyzing, the protein was loaded into a Q Sepharose Fast Flow (Pharmacia), washed with 100 ml Buffer B, and eluted with a 100 ml gradient from 6% Buffer C (20 mM Tris [pH 8.0] and 2 or 10 mM dithiothreitol) to Buffer C + 1 M NaCl. As a last step of purification, the pooled fractions were loaded into a Superdex 75 gel filtration column and eluted with a buffer containing 20 mM TRIS (pH 8.0), 250 mM NaCl, and 2 or 10 mM dithiothreitol. Protein concentration was determined by UV absorption as described (Gill and von Hippel, 1989).

### Crystallization, Data Collection, and Processing

Both crystal forms grew by hanging drop vapor diffusion at 4°C. For the $P4_12_12$ crystals (GMP-bound form), 2 μl of 8 mg/ml protein containing 5 mM GMP was mixed with 1.6 μl of mother liquor, consisting of 100 mM HEPES (pH 7.7) and 50% MPD (2-methyl-2,4-pentanediol), and 0.4 μl of guanidine 1 M on a siliconized glass cover slip and equilibrated against 1.0 ml of mother liquor. Pyramidal crystals grew after 48 hr. For the P1 crystals (apo form), two microliters of 8 mg/ml protein containing 5 mM GMP was mixed with 2.0 μl of mother liquor, consisting of 100 mM MES (pH 6.3) and 60% MPD (2-methyl-2,4-pentanediol), on a siliconized glass cover slip

and equilibrated against 1.0 ml of mother liquor. Rod-shaped crystals grew after a week. Crystals were flash frozen directly in liquid nitrogen-cooled propane.

MAD data were collected using two wavelengths (Table 1) at 100 K at beamline 9.2 at SSRL (Stanford, CA) using a Quantum4 CCD detector. The data acquisition schedule consisted of 15° wedges followed by the corresponding inverse beam wedge at the peak wavelength (0.978996 Å) and then the same reciprocal space wedges at the high-energy remote wavelength (0.904964 Å). Diffraction data were processed using DENZO (Otwinowski and Minor, 1997), and intensities were reduced and scaled using SCALEPACK (Otwinowski and Minor, 1997) (Table 1).

### Structure Determination

The three expected selenium sites for the SeMet GMP-bound crystals were found using an automated Patterson heavy atom search method (Grosse-Kunstleve and Brunger, 1999) in an averaged Patterson map calculated from an anomalous difference Patterson map at the peak wavelength and a dispersive differences Patterson map. Two of the Se sites were well ordered and were included in the heavy atom site refinement against a maximum likelihood target. The f′ and f″ scattering factors were individually refined for each site. Density modification with solvent flipping (Abrahams and Leslie, 1996) and histogram matching (Zhang and Main, 1990) were carried out using the MAD phases with further phase extension to the minimum Bragg spacing of the native dataset. The resulting electron density map was mostly traceable, although some regions only became clear in subsequent phase-combined maps using a partial model. The P1 apo form of the PSD-95 crystals, which had two molecules in the asymmetric unit, was phased through molecular replacement using two models, one for the SH3 domain and one for the GK domain. The two GK domains were unambiguously located, and the SH3 domains were located with the two GK domains already in place. All heavy atom search, phasing, density modification, and molecular replacement calculations were carried out with the Crystallography and NMR System (CNS) (Brunger et al., 1998).

### Model Building and Refinement

The GMP-bound model of PSD-95 was built using the program O (Jones et al., 1991). The resulting density-modified MAD map, in combination with the known Se sites and a number of tryptophan residues, allowed unambiguous tracing for most of the protein backbone and side chain atoms. The refinement of the model was carried out with torsion angle dynamics-simulated annealing (Rice and Brunger, 1994) using the MLHL target function (Pannu et al., 1998), which included the experimental MAD phases prior to solvent flattening as initial phase information in the calculation. The $R_{free}$ (Brunger, 1992), calculated with 10% randomly selected reflections, was used to monitor the refinement and model-building cycles. Model building was done using 2Fo–Fc MAD phase-combined electron density maps using the experimental MAD phases and $\sigma_A$-weighted model phases (Read, 1986) calculated with the annealed model after individual restrained B factor refinement (Hendrickson, 1985). The apo form of PSD-95 was refined against the MLF (Adams et al., 1997) target function using $R_{free}$ to monitor the refinement. Following model building, cycles used $\sigma_A$ electron density maps calculated with the annealed model after individual restrained B factor refinement. Water molecules were added to both structures where chemically reasonable using an automatic procedure in CNS, and the final model for the GMP-bound form of PSD-95 had 87 water molecules, while the apo form contained 188 water molecules. The GMP-bound form presented additional electron density that could be modeled as guanidine (two molecules) and MPD (two molecules). All refinement calculations were carried out with CNS (Brunger et al., 1998) (Table 1).

### Figure Preparation

All figures were prepared using Molscript (Kraulis, 1991) and PyMOL (DeLano, 2001).

### Acknowledgments

We thank C. Stroupe, R.B. Sutton, M. Bowen, J. Ernst, B. Delabarre, J.M. Anderson, and P. de Camilli for critical reading of the manuscript. Portions of this research were carried out at the Stanford Synchrotron Radiation Laboratory, a national user facility operated by Stanford University on behalf of the U.S. Department of Energy, Office of Basic Energy Sciences. The SSRL Structural Molecular Biology Program is supported by the Department of Energy, Office of Biological and Environmental Research, and by the National Institutes of Health, National Center for Research Resources, Biomedical Technology Program, and the National Institute of General Medical Sciences.

Received September 5, 2001; revised November 1, 2001.

### References

Abrahams, J.P., and Leslie, A.G.W. (1996). Methods used in the structure determination of bovine mitochondrial F1 ATPase. Acta Crystallogr. D *52*, 30–42.

Adams, P.D., Pannu, N.S., Read, R.J., and Brunger, A.T. (1997). Cross-validated maximum likelihood enhances crystallographic simulated annealing refinement. Proc. Acad. Sci. USA *94*, 5018–5023.

Anderson, J.M. (1996). Cell signaling: MAGUK magic. Curr. Biol. *6*, 382–384.

Blaszczyk, J., Li, Y., Yan, H., and Ji, X. (2001). Crystal structure of unligated guanylate kinase from yeast reveals GMP-induced conformational changes. J. Mol. Biol. *307*, 247–257.

Brenman, J.E., Topinka, J.R., Cooper, E.C., McGee, A.W., Rosen, J., Milroy, T., Ralston, H.J., and Bredt, D.S. (1998). Localization of postsynaptic density-93 to dendritic microtubules and interaction with microtubule-associated protein 1A. J. Neurosci. *18*, 8805–8813.

Brunger, A.T. (1992). The free R value: a novel statistical quantity for assessing the accuracy of crystal structures. Nature *355*, 472–474.

Brunger, A.T., Adams, P.D., Clore, G.M., Gross, P., Grosse-Kunstleve, R.W., Jiang, J.-S., Kuszewski, J., Nilges, M., Pannu, N.S., Read, R.J., et al. (1998). Crystallography and NMR system (CNS): a new software system for macromolecular structure determination. Acta Crystallogr. D *54*, 905–921.

Cho, K.O., Hunt, C.A., and Kennedy, M.B. (1992). The rat brain postsynaptic density fraction contains a homolog of the *Drosophila* disc-large tumor suppressor protein. Neuron *9*, 929–942.

Cohen, A.R., Woods, D.F., Marfatia, S.M., Walther, Z., Chisti, A.H., and Anderson, J.M. (1998). Human Cask/Lin2 binds syndecan-2 and protein 4.1 and localizes to the basolateral membrane of epithelial cells. J. Cell Biol. *142*, 129–138.

Colledge, M., and Scott, J.D. (1999). AKAPs: from structure to function. Trends Cell Biol. *9*, 216–221.

Colledge, M., Dean, R.A., Scott, G.K., Langeberg, L.K., Huganir, R.L., and Scott, J.D. (2000). Targeting of PKA to glutamate receptors through a MAGUK-AKAP complex. Neuron *27*, 107–119.

Deguchi, M., Hata, Y., Takeuchi, M., Ide, N., Hirao, K., Yao, I., Irie, M., Toyoda, A., and Takai, Y. (1998). BEGAIN (brain-enriched guanylate kinase-associated protein), a novel neuronal PSD-95/SAP90-binding protein. J. Biol. Chem. *273*, 26269–26272.

DeLano, W.L. (2001). The PyMOL Molecular Graphics System (http://www.pymol.org).

Dimitratos, S.D., Woods, D.F., Stathakis, D.G., and Bryant, P.J. (1999). Signaling pathways are focused at specialized regions of the plasma membrane by scaffolding proteins of the MAGUK family. Bioessays *11*, 912–921.

Dodge, K., and Scott, J.D. (2000). AKAP79 and the evolution of the AKAP model. FEBS Lett. *476*, 58–61.

Fanning, A.S., and Anderson, J.M. (1999). Protein modules as organizers of membrane structure. Curr. Opin. Cell Biol. *11*, 432–439.

Garcia, E.P., Mehta, S., Blair, L.A., Wells, D.G., Shang, J., Fukushima, T., Fallon, J.R., Garner, C.C., and Marshall, J. (1998). SAP90 binds and clusters kainite receptors causing incomplete desensitization. Neuron *21*, 727–739.

Gill, S.C., and von Hippel, P.H. (1989). Calculation of protein extinc-

tion coefficients from amino acid sequence data. Anal. Biochem. *182*, 319–326.

Grosse-Kunstleve, R.W., and Brunger, A.T. (1999). A highly automated heavy-atom search procedure for macromolecular structures. Acta Crystallogr. D *55*, 1568–1577.

Hendrickson, W.A. (1985). Stereochemically restrained refinement of macromolecular structures. Methods Enzymol. *115*, 252–270.

Hendrickson, W.A. (1991). Determination of macromolecular structures from anomalous diffraction of synchrotron radiation. Science *254*, 51–58.

Hough, C.D., Woods, D.F., Park, S., and Bryant, P.J. (1997). Organizing a functional junctional complex requires specific domains of the Drosophila MAGUK discs large. Genes Dev. *11*, 3242–3253.

Jones, T.A., Zou, J.Y., Cowan, S.W., and Kjeldgaard, M. (1991). Improved methods for building protein models in electron density maps and the location of errors in these models. Acta Crystallogr. A *47*, 110–119.

Kim, E., Naisbitt, S., Hsueh, Y.-P., Rao, A., Rothschild, A., Craig, A.M., and Sheng, M. (1997). GKAP, a novel synaptic protein that interacts with the guanylate kinase-like domain of the PSD-95/SAP90 family of channel clustering molecules. J. Cell Biol. *136*, 669–678.

Kistner, U., Wenzel, B.M., Veh, R.W., Cases-Langhoff, C., Garner, A.M., Appletauer, U., Voss, B., Gundelfinger, E.D., and Garner, C.C. (1993). SAP90, a rat presynaptic protein related to the product of the Drosophila tumor suppressor gene *dlg*-A. J. Biol. Chem. *268*, 4580–4583.

Kistner, U., Garner, C.C., and Linial, M. (1995). Nucleotide binding by the synapse associated protein SAP90. FEBS Lett. *359*, 159–163.

Kraulis, P. (1991). MOLSCRIPT: a program to produce both detailed and schematic plots of protein structures. J. Appl. Crystallogr. *24*, 946–950.

Kuhlendahl, S., Spangenberg, O., Konrad, M., Kim, E., and Garner, C.C. (1998). Functional analysis of the guanylate kinase-like domain in the synapse-associated protein SAP97. Eur. J. Biochem. *252*, 305–313.

Lue, R.A., Marfatia, S.M., Branton, D., and Chisti, A.H. (1994). Cloning and characterization of hdlg: the human homologue of the *Drosophila* discs large tumor suppressor binds to protein 4.1. Proc. Natl. Acad. Sci. USA *91*, 9818–9822.

Lüscher, C., Nicoll, R.A., Malenka, R.C., and Muller, D. (2000). Synaptic plasticity and dynamic modulation of the postsynaptic membrane. Nature Neurosci. *3*, 545–550.

Marfatia, S.M., Lue, R.A., Branton, D., and Chisti, A.H. (1994). *In vitro* binding studies suggest a membrane-associated complex between erythroid p55, protein 4.1, and glycophorin C. J. Biol. Chem. *269*, 8631–8634.

Masuko, N., Makino, K., Kuwahara, H., Fukunaga, K., Sudo, T., Araki, N., Yamamoto, H., Yamada, Y., Miyamoto, E., and Saya, H. (1999). Interaction of NE-dlg/SAP102, a neuronal and endocrine tissue-specific membrane-associated guanylate kinase protein, with calmodulin and PSD-95/SAP90. J. Biol. Chem. *274*, 5782–5790.

McGee, A.W., and Bredt, D.S. (1999). Identification of an intramolecular interaction between the SH3 and guanylate kinase domains of PSD-95. J. Biol. Chem. *274*, 17431–17436.

Meador, W.E., Means, A.R., and Quiocho, F.A. (1992). Target enzyme recognition by calmodulin: 2.4 Å structure of a calmodulin-peptide complex. Science *257*, 1251–1255.

Migaud, M., Charlesworth, P., Dempster, M., Webster, L.C., Watabe, A.M., Makhisnson, M., He, Y., Ramsay, M.F., Morris, R.G.M., Morrison, J.H., et al. (1998). Enhanced long-term potentiation and impaired learning in mice with mutant postsynaptic density-95 protein. Nature *396*, 433–439.

Naisbitt, S., Kim, E., Weinberg, R.J., Rao, A., Yang, F.-C., Craig, A.M., and Sheng, M. (1997). Characterization of guanylate kinase-associated protein, a postsynaptic density protein at excitatory synapses that interacts directly with postsynaptic density-95/synapse-associated protein 90. J. Neurosci. *17*, 5687–5696.

Nicholls, A., Bharadwaj, R., and Honig, B. (1993). GRASP: graphical representation and analysis of surface properties. Biophys. J. *64*, A166.

Nix, S.L., Chisti, A.H., Anderson, J.M., and Walther, Z. (2000). HCASK and hDlg associate in epithelia, and their Src homology 3 and guanylate kinase domains participate in both intramolecular and intermolecular interactions. J. Biol. Chem. *275*, 41192–41200.

Otwinowski, Z., and Minor, W. (1997). Processing of X-ray diffraction data collected in oscillation mode. Methods Enzymol. *276*, 307–326.

Pannu, N.S., Murshudov, G.N., Dodson, E.J., and Read, R.J. (1998). Incorporation of prior phase information strengthens maximum-likelihood structure refinement. Acta Crystallogr. D *54*, 1285–1294.

Pak, D.T.S., Yang, S., Rudolph-Correia, S., Kim, E., and Sheng, M. (2001). Regulation of dendritc spine morphology by SPAR, a PSD-95-associated RapGAP. Neuron *31*, 289–303.

Pawson, T., and Scott, J.D. (1997). Signaling through scaffold, anchoring, and adaptor proteins. Science *278*, 2075–2080.

Read, R.J. (1986). Improved Fourier coefficients for maps using phases from partial structures with errors. Acta Crystallogr. A *42*, 140–149.

Rhoads, A.R., and Friedberg, F. (1997). Sequence motifs for calmodulin recognition. FASEB J. *11*, 331–340.

Rice, L.M., and Brunger, A.T. (1994). Torsion angle dynamics: reduced variable conformational sampling enhances crystallographic structure refinement. Proteins *19*, 277–290.

Scannevin, R.H., and Huganir, R.L. (2000). Postsynaptic organization and regulation of excitatory synapses. Nature Reviews *1*, 133–141.

Sheng, M., and Pak, D.T.S. (2000). Ligand-gated ion channel interactions with cytoskeletal and signaling proteins. Annu. Rev. Physiol. *62*, 755–778.

Shin, H., Hsueh, Y.-P., Yang, F.-C., Kim, E., and Sheng, M. (2000). An intramolecular interaction between Src homology 3 domain and guanylate kinase-like domain required for channel clustering by postsynaptic density-95/SAP90. J. Neurosci. *20*, 3580–3587.

Sicheri, F., Moarefi, I., and Kuriyan, J. (1997). Crystal structure of the Src family tyrosine kinase Hck. Nature *385*, 602–609.

Stathakis, D.G., Hoover, K.B., You, Z., and Bryant, P.J. (1997). Human postsynaptic density-95 (PSD-95): location of the gene (DLG4) and possible function in nonneural as well as in neural tissues. Genomics *44*, 71–82.

Takeuchi, M., Hata, Y., Hirao, K., Toyoda, A., Irie, M., and Takai, Y. (1997). SAPAPs a family of PSD-95/SAP90-associated proteins localized at postsynaptic density. J. Biol. Chem. *272*, 11943–11951.

Thomas, U., Ebitsch, S., Gorczyca, M., Koh, Y.H., Hough, C.D., Woods, D., Gundelfinger, E.D., and Budnik, V. (2000). Synaptic targeting and localization of Discs-large is a stepwise process controlled by different domains of the protein. Curr. Biol. *10*, 1108–1117.

Thompson, J.D., Higgins, D.G., and Gibson, T.J. (1994). CLUSTALW: improving the sensitivity of progressive multiple sequence alignment through sequence weighting, positions specific gap penalties and weight matrix choice. Nucleic Acids Res. *22*, 4673–4680.

Tomita, S., Nicoll, R.A., and Bredt, D.S. (2001). PDZ protein interactions regulating glutamate receptor function and plasticity. J. Cell Biol. *153*, F19–F23.

Woods, D.F., and Bryant, J.P. (1993). ZO-1, DlgA and PSD-95/SAP90: homologous proteins in tight, septate and synaptic cell junctions. Mech. Dev. *44*, 85–89.

Woods, D.F., Hough, C., Peel, D., Callaini, G., and Bryant, J.P. (1996). Dlg protein is required for junction structure, cell polarity, and proliferation control in Drosophila epithelia. J. Cell Biol. *134*, 1469–1482.

Wu, H., Reissner, C., Kuhlendahl, S., Coblentz, B., Reuver, S., Kindler, S., Gundelfinger, E.D., and Garner, C.C. (2000). Intramolecular interactions regulate SAP97 binding to GKAP. EMBO J. *19*, 5740–5751.

Xu, W., Harrison, S.C., and Eck, M.J. (1997). Three-dimensional structure of the tyrosine kinase c-Src. Nature *385*, 595–601.

Zhang, K.Y.J., and Main, P. (1990). Histogram matching as a new density modification technique for phase refinement and extension of protein molecules. Acta Crystallogr. A *46*, 41–46.

Ziff, E.B. (1997). Enlightening the postsynaptic density. Neuron *19*, 1163–1174.

**Accession Numbers**

The apo and GMP-bound forms have been deposited with ID codes 1JXO and 1JXM, respectively.